

Majorana fermions from Landau quantization in a superconductor–topological-insulator hybrid structure

Rakesh P. Tiwari,¹ U. Zülicke,² and C. Bruder¹

¹*Department of Physics, University of Basel, Klingelbergstrasse 82, CH-4056 Basel, Switzerland*

²*School of Chemical and Physical Sciences and MacDiarmid Institute for Advanced Materials and Nanotechnology, Victoria University of Wellington, PO Box 600, Wellington 6140, New Zealand*

(Dated: October 16, 2012)

We show that the interplay of cyclotron motion and Andreev reflection experienced by massless-Dirac-like charge carriers in topological-insulator surface states generates a Majorana-particle excitation. Based on an envelope-function description of the Dirac-Andreev edge states, we discuss the kinematic properties of the Majorana mode and find them to be possible to be tuned by changing the superconductor's chemical potential and/or the magnitude of the perpendicular magnetic field. Our proposal opens up new possibilities for studying Majorana fermions in a controllable setup.

PACS numbers: 73.20.At, 73.25.+i, 74.45.+c, 73.50.Jt

Introduction. – In recent years, the possibility of observing and exploiting Majorana quasiparticles in condensed matter systems has attracted a great deal of attention [1–4]. Originally these elusive fermionic particles were proposed as real solutions of the Dirac equation [5]. Potential condensed-matter systems hosting realizations of these atypical fermions include the $\nu = 5/2$ quantum-Hall state [6, 7], p -wave superconductors [8] such as strontium ruthenate [9], semiconductor-superconductor heterostructures [10–12] and the surface of topological insulators [13, 14] among others. An experimental signature of localized Majorana excitations are zero-bias conductance anomalies [15–18] that may have been measured recently [19, 20].

A particularly interesting route towards realizing chiral Majorana modes involves hybrid structures of a topological insulator (TI) and an s -wave superconductor [21, 22]. The requirement of broken time-reversal symmetry and gapped excitation spectrum for the surface states in the TI could be fulfilled by proximity to a ferromagnetic insulator [22] or Zeeman splitting due to a magnetic field [21]. Here we pursue an alternative scenario where Landau quantization of the surface states' orbital motion in a uniform perpendicular magnetic field is the origin of a gap and breaking of time-reversal symmetry. Besides avoiding materials-science challenges associated with fabrication of hybrid structures involving three different kinds of materials, our setup also offers several new features enabling the manipulation of the Majorana excitation's properties.

Figure 1 illustrates the proposed sample geometry. The massless-Dirac-like surface states of a bulk three-dimensional TI material (e.g., Bi_2Se_3 [13]) occupy the xy plane. A planar contact with a superconductor in the half-plane $x < 0$ induces a pair potential for this part of the TI surface (henceforth called the S region), while a uniform perpendicular magnetic field $\mathbf{B} = B\hat{z}$ is present in the half-plane $x > 0$ (the N region of the TI surface). We assume the magnetic field to be fully screened from the S part and neglect Zeeman splitting

throughout [23]. The interplay of cyclotron motion of charge carriers in the N region with Andreev reflection from the interface with the S region results in the formation of chiral Dirac-Andreev edge states similar to the ones discussed previously for an S–graphene hybrid structure [24]. The quantum description of these edge channels reveals one of them to be associated with a chiral Majorana fermion mode with tunable velocity and guiding-center-dependent electric charge.

Basic model for the S–TI hybrid structure. – To describe single-particle excitations in the S–N heterostructure made from TI surface states, we employ the Dirac-Bogoliubov-de Gennes (DBdG) equation [21, 24]

$$\begin{pmatrix} H_D(\mathbf{r}) - \mu & \Delta(\mathbf{r})\sigma_0 \\ \Delta^*(\mathbf{r})\sigma_0 & \mu - TH_D(\mathbf{r})T^{-1} \end{pmatrix} \Psi(\mathbf{r}) = \varepsilon\Psi(\mathbf{r}), \quad (1)$$

with the pair potential $\Delta(\mathbf{r}) = e^{i\phi}\Delta_0\Theta(-x)$ finite only in the S region, $\sigma_0 \equiv \mathbb{1}_{2\times 2}$ denoting the two-dimensional identity matrix, and $H_D(\mathbf{r}) = v_F[\mathbf{p} + e\mathbf{A}(\mathbf{r})] \cdot \boldsymbol{\sigma}$ being the massless-Dirac Hamiltonian for the TI surface states. The position $\mathbf{r} \equiv (x, y)$ and momentum $\mathbf{p} \equiv -i\hbar(\partial_x, \partial_y)$

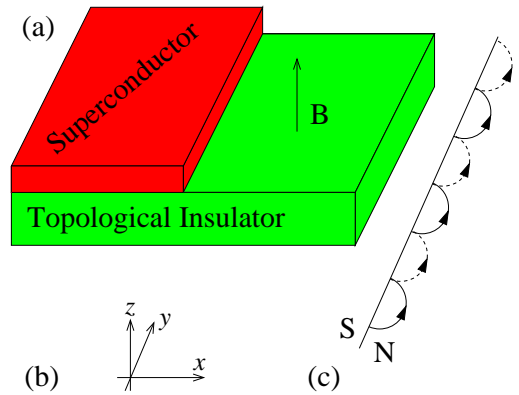


FIG. 1. (Color online) (a) Schematics of the proposed sample layout. (b) The coordinate system. (c) The semiclassical picture of Dirac-Andreev edge states (solid and dashed lines represent electrons and holes respectively).

are restricted to the TI surface, σ is the vector of Pauli matrices acting in spin space. Furthermore, T denotes the time-reversal operator, $-e$ the electron charge, and \mathbf{A} the vector potential associated with the magnetic field $\mathbf{B} = \nabla \times \mathbf{A}$. The excitation energy ε is measured relative to the chemical potential μ of the superconductor, with the absolute zero of energy set to be at the Dirac (i.e., neutrality) point of the TI surface states. The wave function Ψ from Eq. (1) is a spinor in Dirac-Nambu space, which can be expressed explicitly in terms of spin-resolved amplitudes as $\Psi = (u_\uparrow, u_\downarrow, v_\downarrow, -v_\uparrow)^T$.

To describe the uniform perpendicular magnetic field in the N region, we adopt the Landau gauge $\mathbf{A} = Bx\hat{\mathbf{y}}$. Then the momentum $\hbar q$ parallel to the interface (i.e., in $\hat{\mathbf{y}}$ direction) is a good quantum number of the DBdG Hamiltonian, and a general eigenspinor is of the form

$$\Psi_{nq}(\mathbf{r}) = e^{\frac{i\phi}{2}\sigma_0 \otimes \tau_z} e^{iqy} \Phi_{nq}(x). \quad (2)$$

Here τ_z is a Pauli matrix acting in Nambu space, σ_0 the identity in spin space, and n enumerates the energy (Landau) levels for a fixed q . The spinors $\Phi_{nq}(x)$ are solutions of the one-dimensional (1D) DBdG equation $\mathcal{H}(q)\Phi_{nq}(x) = \varepsilon\Phi_{nq}(x)$, with

$$\mathcal{H}(q) = \hbar v_F \left\{ \sigma_x \otimes \tau_z (-i) \partial_x + \sigma_y \otimes \left[\tau_z q + \tau_0 \frac{eB}{\hbar} x \Theta(x) \right] \right\} - \mu \sigma_0 \otimes \tau_z + \Delta_0 \Theta(-x) \sigma_0 \otimes \tau_x \quad (3)$$

where the τ_j are Pauli matrices acting in Nambu space, and τ_0 the identity in Nambu space. A calculation similar to the one performed in Ref. 24 yields the spectrum of Landau-level (LL) eigenenergies ε_{nq} and explicit expressions for $\Phi_{nq}(x)$ in the N and S regions (see the Supplemental Material [25], part A, for more details). When $\mu \neq 0$, a finite dispersion near $q = 0$ is exhibited (see Fig. 2 that also shows the dispersionless Landau levels corresponding to $\mu = 0$), which indicates the emergence of chiral Andreev edge channels [24, 26] that are localized near the interface between the S and N regions.

Emergence of the Majorana mode. – We now examine in greater detail the states associated with the linearly dispersing part of the $n = 0$ level. A general symmetry property [27] of the DBdG equation mandates that, for any eigenstate Ψ_{nq} with excitation energy ε_{nq} , its particle-hole conjugate $\Xi \Psi_{nq}$ in Nambu space [28] is also an eigenstate and has excitation energy $-\varepsilon_{nq}$. This symmetry implies that the state with quantum numbers $n = 0$ and $q = 0$ is its own particle-hole conjugate, thus exhibiting the defining property of a Majorana fermion [1, 2, 5]. Explicit inspection indeed verifies the relation $\Xi \Psi_{00}(\mathbf{r}) = -i \Psi_{00}(\mathbf{r})$ (see the Supplemental Material [25], part B, for more details).

While the Majorana state $\Psi_{00}(\mathbf{r})$ has a localized spatial profile in the direction perpendicular to the S–N junction (i.e., the x -direction), it is completely delocalized in the direction parallel to the S–N junction. To explore this Majorana mode further, we have developed a description of single-particle excitations with $q \neq 0$ based on an adaptation of the envelope-function (EF) theory commonly applied in semiconductor physics [29]. A general eigenstate of the Hamiltonian $\mathcal{H}(q)$ can be expressed in terms of the eigenstates at $q = 0$ as

$$\Phi_{nq}(x) = \sum_{n'} a_{nq}^{(n')} \Phi_{n'0}(x). \quad (4)$$

Inserting this expansion into the 1D DBdG equation and

projecting onto specific basis states $\Phi_{n''0}$ yields a set of linear equations $\sum_{n'} \mathcal{H}_{n''n'}^{(\text{EF})}(q) a_{nq}^{(n')} = \varepsilon a_{nq}^{(n')}$ for the coefficients, in the process defining the general EF matrix

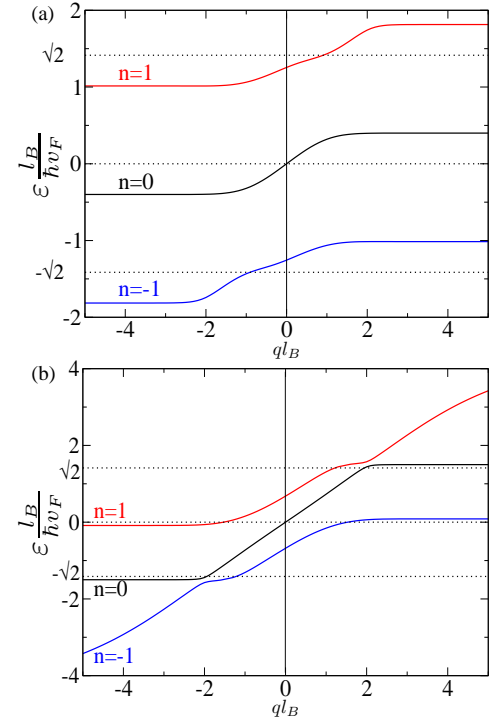


FIG. 2. (Color online) Dispersion relation ε_{nq} of single-particle excitations at the S–N junction on a TI's surface and subject to a strong perpendicular magnetic field. Landau levels with $n = 0, \pm 1$ are shown for $\Delta_0 = 5\hbar v_F/l_B$ and $\mu = 0.4\hbar v_F/l_B$ [panel (a)], $\mu = 1.5\hbar v_F/l_B$ [panel (b)], and $\mu = 0$ (dotted lines). $l_B \equiv \sqrt{\hbar/|eB|}$ is the magnetic length.

Hamiltonian

$$\mathcal{H}_{n''n'}^{(\text{EF})}(q) = \varepsilon_{n'0} \delta_{n'n''} + \int_{-\infty}^{\infty} dx [\Phi_{n''0}(x)]^\dagger \{\mathcal{H}(q) - \mathcal{H}(0)\} \Phi_{n'0}(x) \quad (5)$$

Specializing to the 1D DBdG Hamiltonian, we find

$$\mathcal{H}(q) - \mathcal{H}(0) = \hbar v_F q \sigma_y \otimes \tau_z \equiv q \left[\frac{\partial \mathcal{H}(q)}{\partial q} \right]_{q=0}, \quad (6)$$

which is independent of spatially varying quantities (the vector and pair potentials). Application of the Hellmann-Feynman theorem [30] facilitates further calculation of the EF matrix Hamiltonian (see the Supplemental Material [25], part E, for more details). With mode-dependent velocities

$$v_n \equiv \frac{1}{\hbar} \frac{\partial \varepsilon_{nq}}{\partial q} \Big|_{q=0} = v_F \int_{-\infty}^{\infty} dx [\Phi_{n0}(x)]^\dagger \sigma_y \otimes \tau_z \Phi_{n0}(x), \quad (7)$$

we finally obtain an expression where intra-LL and inter-LL couplings are neatly separated:

$$H_{n''n'}^{(\text{EF})}(q) = (\varepsilon_{n'0} + \hbar v_{n'} q) \delta_{n'n''} + q (\varepsilon_{n'0} - \varepsilon_{n''0}) A_{n''n'}, \quad (8a)$$

$$A_{n''n'} = \int_{-\infty}^{\infty} dx [\Phi_{n''0}(x)]^\dagger \left[\frac{\partial}{\partial q} \Phi_{n'q}(x) \right]_{q=0}. \quad (8b)$$

The EF approach is particularly useful to consider states with small $q \lesssim l_B^{-1}$, as it provides a natural platform for a perturbative treatment. To lowest (i.e., linear) order in q , the dispersion of the $n = 0$ Dirac-Andreev edge state is given by $\varepsilon_{0q} = \hbar v_0 q + \mathcal{O}(q^2)$, and the second-quantized particle annihilation operator for the state with $n = 0$ and finite small q is found to be

$$\gamma_q = c_0 + q \sum_{n>0} A_{n0} (c_n - c_n^\dagger) + \mathcal{O}(q^2). \quad (9)$$

The c_j in Eq. (9) are single-particle operators associated with the EF basis states $\Phi_{j0}(x)$, satisfying the usual fermionic anticommutation relations, and $c_0^\dagger = c_0$. The structure of the expression (9) embodies the relation

$$\gamma_q^\dagger = \gamma_{-q}, \quad (10)$$

which fundamentally arises as a consequence of particle-hole symmetry in the DBdG equation. The identity (10) is a hallmark of a Majorana excitation [22], because it enables construction of a real-space particle operator [31]

$$\gamma_\Lambda(y) = \mathcal{N}_\Lambda \int_{-\Lambda}^{\Lambda} dq e^{iqy} \gamma_q \quad (11)$$

that satisfies the condition $\gamma_\Lambda(y)^\dagger = \gamma_\Lambda(y)$.

Majorana fermions are often also called ‘half-fermions’ because an ordinary (complex, Dirac) electron can be considered to be made up of two Majorana (real) fermion

degrees of freedom with perfectly synchronized dynamics. Thus the emergence of independent Majorana excitations in an electronic system is often due to the fractionalization of an ordinary electron state, brought about by complex correlations in a material’s electronic ground state. Naturally, a fractionalization scenario always generates pairs of free Majorana excitations, and the physical separation of the constituents of the pair has to be ensured to avoid their ‘recombination’ into an ordinary electron. The breaking of time-reversal symmetry due to the applied magnetic field eliminates the possibility for there to be a doubly occupied zero-energy state at $x = 0$ with guiding center $q = 0$. As particle-hole symmetry is preserved, such a state has to be a chiral Majorana excitation. There is no partner-complement along the NS-interface $x = 0$ to form a Dirac fermion, hence this excitation will be stable (e.g. against disorder) as long as a zero-energy state can exist.

Electric charge of Dirac-Andreev edge states. As is the case for Bogoliubov quasiparticles in a conventional superconductor [27, 32–35], the Dirac-Andreev edge states are coherent superpositions of particles and holes in Nambu space. Consequently, their effective electric charge generally has a non-quantized value

$$e^{(\Psi)} = \int d^2r [\Psi(\mathbf{r})]^\dagger \sigma_0 \otimes \tau_z \Psi(\mathbf{r}) \quad (12)$$

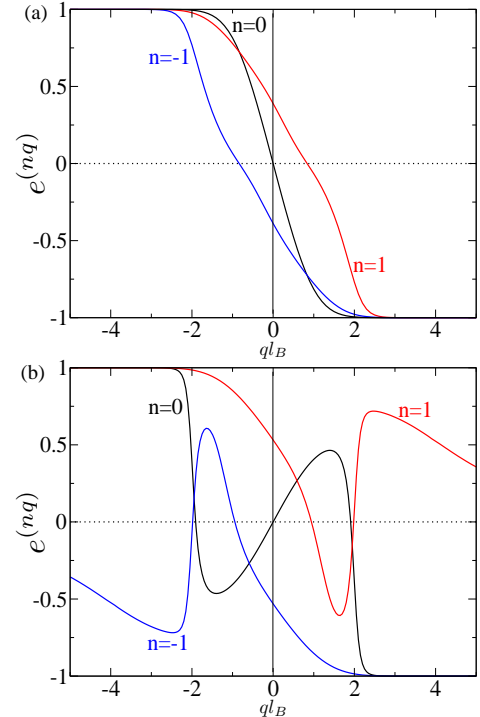


FIG. 3. (Color online) Effective electric charge $e^{(nq)}$ of the single-particle excitations for the parameters used in Figs. 2a and b, numerically calculated using the normal-side wavefunctions in Eq. (12). For both sets of parameters, $e^{(00)} = 0$ as expected for a Majorana state. Notice also the linear variation of $e^{(nq)}$ for small $q \lesssim l_B^{-1}$.

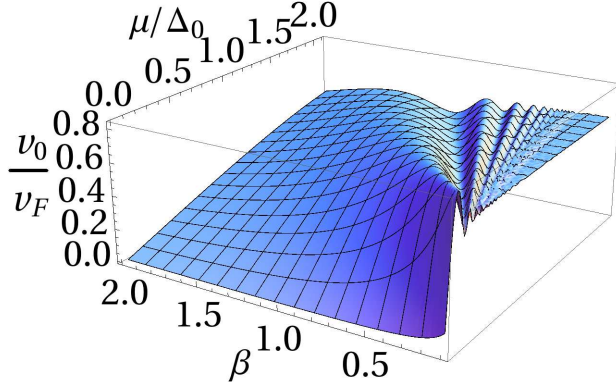


FIG. 4. (Color online) Dependence of the Majorana-mode velocity v_0 on system parameters. $\beta = \sqrt{\hbar|eB|}v_F/\Delta_0$ measures the magnetic-field strength, μ is the superconductor's chemical potential, and Δ_0 the magnitude of the superconducting pair potential.

that depends on the particular state. Figure 3 shows the numerically calculated charges $e^{(nq)}$ of states from the bands $n = 0, \pm 1$ given in Fig. 2.

Using the EF theory discussed above, we can express the charge of modes with small $q \neq 0$ as

$$e^{(nq)} = e_{nn} + 2q \operatorname{Re} \sum_{n' \neq n} A_{n'n} e_{n'n} + \mathcal{O}(q^2), \quad (13a)$$

with the basis-function-related charge parameters

$$e_{n'n} = \int dx [\Phi_{n'0}(x)]^\dagger \sigma_0 \otimes \tau_z \Phi_{n0}(x). \quad (13b)$$

By definition, $e_{nn} \equiv e^{(n0)}$ is the effective charge of the EF basis state with quantum number n . The q -proportional coupling of basis states results in a linear q dependence of e_{nq} for $q \lesssim l_B^{-1}$, in agreement with Fig. 3.

For the $n = 0$ (Majorana) mode, $e^{(0,-q)} = -e^{(0q)}$ and, as expected, the state at $q = 0$ has zero effective charge. A general superposition $\Psi_0(\mathbf{r}) \equiv \sum_{|q| < \Lambda} \alpha_q \Psi_{0q}(\mathbf{r})$ of Majorana-mode states has total electric charge

$$e^{(\Psi_0)} = \frac{\langle \varepsilon \rangle}{\hbar v_0} \left. \frac{\partial e^{(0q)}}{\partial q} \right|_{q=0} \quad (14)$$

proportional to its mean energy $\langle \varepsilon \rangle \equiv \sum_{|q| < \Lambda} |\alpha_q|^2 \varepsilon_{0q}$. Thus the Majorana mode's energy relaxation will be associated with charge conversion, which is a general feature for bogolon excitations in superconductors [32, 35]. Furthermore, as the superposition associated with the real-space Majorana-particle operator $\gamma_\Lambda(y)$ involves states

with $\pm q$ in equal measure, its total charge vanishes as is expected for a true Majorana fermion. An experimental verification of this property can possibly be done along similar lines as used in recent experiments on edge-magnetoplasmonic excitations in graphene [36] and open up possibilities for electrically manipulating this mode.

Tailoring Majorana-mode properties. – An interesting feature of this realization of a Majorana mode is that its velocity can be tuned via the external magnetic field. This enables a potentially easier route towards tailoring this characteristic property than changing the magnetization of a ferromagnetic insulator in structures of the type discussed in Ref. 22. The mode-velocity dependence on the external magnetic field and the chemical potential is shown in Fig. 4. Furthermore, the charge within the $n = 0$ Landau level can be controlled via the chemical potential. This is evident by comparing the slopes of $e^{(nq)}$ at $q = 0$ in the two panels in Fig. 3.

Conclusions. – We have demonstrated that a Majorana mode can be realized using the interplay of Landau quantization and Andreev reflection in a superconductor–topological-insulator hybrid structure. This mode is robust against disorder due to its chiral nature and associated uniqueness of the zero-energy state that is localized at the interface, and its velocity is tunable by adjusting the strength of the magnetic field. We have developed a theory to describe the coupling of this mode to other Dirac-Andreev edge states and showed how this coupling results in an energy-dependent electric charge for Majorana-mode states. This feature should enable creation and manipulation of such excitations using external gate voltages.

Acknowledgments. – We acknowledge financial support by the Swiss SNF, the NCCR Nanoscience, and the NCCR Quantum Science and Technology.

Appendix A: DBdG eigenspinors in the N region

To simplify the notation we measure all energies in units of $\hbar v_F/l_B$ and lengths in units of l_B . The superconducting pair potential is in general, a complex quantity $\Delta = \Delta_0 e^{i\phi}$. To have a transparent picture of the relative phase between the electronic and the hole excitations we make the ansatz $\Psi(x, y) = e^{iqy} (u_\uparrow(x) e^{i\phi/2}, u_\downarrow(x) e^{i\phi/2}, v_\downarrow(x) e^{-i\phi/2}, -v_\uparrow(x) e^{-i\phi/2})^T$ and obtain a one-dimensional DBdG equation whose solutions that decay for $x \rightarrow \infty$ in region $x > 0$ have the form

$$\Psi(x, y) = e^{iqy} \begin{pmatrix} -iC_e e^{-\frac{(x+q)^2}{2}} (\mu + \varepsilon) H_{(\mu+\varepsilon)^2/2-1}(x+q) e^{i\phi/2} \\ C_e e^{-\frac{(x+q)^2}{2}} H_{(\mu+\varepsilon)^2/2}(x+q) e^{i\phi/2} \\ C_h e^{-\frac{(x-q)^2}{2}} H_{(\mu-\varepsilon)^2/2}(x-q) e^{-i\phi/2} \\ -iC_h e^{-\frac{(x-q)^2}{2}} (\mu - \varepsilon) H_{(\mu-\varepsilon)^2/2-1}(x-q) e^{-i\phi/2} \end{pmatrix}, \quad (\text{A1})$$

with $H_\alpha(x)$ denoting the Hermite function [24]. The complete solution is then obtained by demanding the conservation of particle current along the boundary. Similar to Ref. [24] we find

$$C_e = \frac{-iC_h(\mu - \varepsilon)H_{(\mu-\varepsilon)^2/2-1}(-q)}{H_{(\mu+\varepsilon)^2/2}(q)\frac{\varepsilon}{\Delta_0} + (\mu + \varepsilon)H_{(\mu+\varepsilon)^2/2-1}(q)\sqrt{1 - \frac{\varepsilon^2}{\Delta_0^2}}}, \quad (\text{A2})$$

and the dispersion relation is given by the solutions of

$$f_{\mu+\varepsilon}(q) - f_{\mu-\varepsilon}(-q) = \frac{\varepsilon(f_{\mu+\varepsilon}(q)f_{\mu-\varepsilon}(-q) + 1)}{\sqrt{\Delta_0^2 - \varepsilon^2}},$$

$$f_\alpha(q) = \frac{H_{\alpha^2/2}(q)}{\alpha H_{\alpha^2/2-1}(q)}. \quad (\text{A3})$$

The solutions $\varepsilon_n(q)$ of Eq. (A3) can be labeled with a Landau level (LL) index $n = 0, \pm 1, \pm 2, \dots$. Figure 2(a) in the main text shows the zeroth LL ($n = 0$), along with the neighboring $n = \pm 1$ LLs when $\mu = 0.4\hbar v_F/l_B$ and $\Delta = 5\hbar v_F/l_B$. The dotted lines at $0, \pm\sqrt{2}$ show the dispersionless LLs corresponding to $\mu = 0$. The various levels saturate at $\sqrt{2}(\hbar v_F/l_B)\text{sgn}(n)\sqrt{|n|} - \mu$ for $q \rightarrow -\infty$ and $\sqrt{2}(\hbar v_F/l_B)\text{sgn}(n)\sqrt{|n|} + \mu$ for $q \rightarrow \infty$. This suggests that an interesting regime can be reached by increasing μ , so that $n = \pm 1$ levels start contributing to the low energy excitations of the system. When

the chemical potential μ is finite (as measured from the charge-neutrality point of the free Dirac system), the LLs acquire a dispersion around $q = 0$ that signals the existence of Andreev edge excitations [24, 26].

Appendix B: Verification of Ψ_{00} as a Majorana state

For $\varepsilon = 0$ and $q = 0$ we get $C_h = iC_e$, and this zero energy state can be expressed as

$$\Psi_{00}(x) = C_e e^{-\frac{x^2}{2}} \begin{pmatrix} -i\mu H_{\mu^2/2-1}(x) e^{i\phi/2} \\ H_{\mu^2/2}(x) e^{i\phi/2} \\ iH_{\mu^2/2}(x) e^{-i\phi/2} \\ \mu H_{\mu^2/2-1}(x) e^{-i\phi/2} \end{pmatrix}. \quad (\text{B1})$$

The particle-hole conjugation operator is given by $\Xi = \sigma_y \tau_y \mathcal{K}$ [21], where σ and τ are Pauli matrices acting on spin and particle-hole space respectively, and \mathcal{K} is complex conjugation. Straightforward verification implies $\Xi\Psi_{00} = -i\Psi_{00}$, and $\Xi\Xi\Psi_{00} = \Psi_{00}$. Hence the state Ψ_{00} is a Majorana fermion.

Appendix C: DBdG eigenspinors in the S region

In the superconducting region $x < 0$ the solutions of Eq. (1) in the main text take the form [40]

$$\Psi(x, y) = A e^{iqy} e^{ik_0 x} e^{\kappa x} \begin{pmatrix} e^{-i\theta} e^{i\phi/2} \\ e^{i\gamma} e^{-i\theta} e^{i\phi/2} \\ e^{-i\phi/2} \\ e^{i\gamma} e^{-i\phi/2} \end{pmatrix} + B e^{iqy} e^{-ik_0 x} e^{\kappa x} \begin{pmatrix} e^{i\theta} e^{i\phi/2} \\ -e^{-i\gamma} e^{i\theta} e^{i\phi/2} \\ e^{-i\phi/2} \\ -e^{-i\gamma} e^{-i\phi/2} \end{pmatrix}, \quad (\text{C1})$$

where the parameters $\theta, \gamma, k_0, \kappa$ are defined by

$$\theta = \begin{cases} \cos^{-1} \frac{\varepsilon}{\Delta_0} & \text{if } \varepsilon < \Delta_0 \\ -i \cosh^{-1} \frac{\varepsilon}{\Delta_0} & \text{if } \varepsilon > \Delta_0 \end{cases}, \quad (\text{C2})$$

and $\gamma = \sin^{-1} \frac{q}{\mu}$, $k_0 = \sqrt{\mu^2 - q^2}$, $\kappa = \frac{\mu\Delta_0}{k_0} \sin(\theta)$.

It should be noted that the solutions of the DBdG Hamiltonian given by Eq. (C1), are approximate solutions valid in the regime $\mu \gg \Delta_0, \varepsilon$ for all values of q . We are interested in the eigenstate at $q = 0$ where Eq. (C1) represents an exact solution.

The coefficients A, B, C_e , and C_h can be obtained by demanding the continuity of the wavefunction at $x =$

0 [24]. Due to translational invariance in the y direction, the wavefunction matching can be done for each q separately. Thus we obtain (for $q = 0$ and $\varepsilon = 0$)

$$\begin{aligned} -iA + iB &= C_e(-i)\mu H_{\mu^2/2-1}(0), \\ -iA - iB &= C_e H_{\mu^2/2}(0), \\ A + B &= C_h H_{\mu^2/2}(0), \\ A - B &= C_h(-i)\mu H_{\mu^2/2-1}(0). \end{aligned} \quad (\text{C3})$$

Once again we obtain $C_h = iC_e$. The eigenspinor for the Majorana state for $x > 0$ is given by Eq. (B1), while for

$x < 0$ it is

$$\Psi_{00}(x) = e^{\Delta_0 x} \begin{pmatrix} (-iAe^{i\mu x} + iBe^{-i\mu x})e^{i\phi/2} \\ (-iAe^{i\mu x} - iBe^{-i\mu x})e^{i\phi/2} \\ (Ae^{i\mu x} + Be^{-i\mu x})e^{-i\phi/2} \\ (Ae^{i\mu x} - Be^{-i\mu x})e^{-i\phi/2} \end{pmatrix}, \quad (C4)$$

where

$$A = \frac{C_e}{2}(\mu H_{\mu^2/2-1}(0) + iH_{\mu^2/2}(0)),$$

$$B = \frac{C_e}{2}(-\mu H_{\mu^2/2-1}(0) + iH_{\mu^2/2}(0)). \quad (C5)$$

Once again we can verify that the state is its own particle-hole conjugate. Thus we have obtained the state

representing the Majorana fermion in first-quantized form in the entire space.

Appendix D: Calculation of the envelope-function Hamiltonian using Eq. (5)

Using the explicit expressions for the eigenstates given by Eqs. (A1) and (C1) we can write the EF matrix Hamiltonian as

$$\mathcal{H}_{n''n'}^{(\text{EF})}(q) = \varepsilon_{n'0}\delta_{n'n''} + \hbar v_F q \mathcal{B}_{n''n'}, \quad (D1)$$

where

$$\mathcal{B}_{n''n'} = \sqrt{N(\varepsilon_{n'0})N(\varepsilon_{n''0})} [2^{\frac{(\mu+\varepsilon_{n'0})^2+(\mu+\varepsilon_{n''0})^2}{2}-1} \pi (g(\varepsilon_{n'0}, \varepsilon_{n''0}) + g(\varepsilon_{n''0}, \varepsilon_{n'0})) + G(\varepsilon_{n'0}, \varepsilon_{n''0}) 2^{\frac{(\mu+\varepsilon_{n'0})^2+(\mu+\varepsilon_{n''0})^2}{2}-1} \pi (g(-\varepsilon_{n'0}, -\varepsilon_{n''0}) + g(-\varepsilon_{n''0}, -\varepsilon_{n'0}))]. \quad (D2)$$

The various functions $N(\eta)$, $g(\eta, \zeta)$, and $G(\eta, \zeta)$ can be expressed using Gamma functions:

$$N(\eta) = \frac{2^{\frac{(\mu+\eta)^2}{2}}\sqrt{\pi}}{4} \left(\frac{\psi(\frac{1}{2} - \frac{(\mu+\eta)^2}{4}) - \psi(-\frac{(\mu+\eta)^2}{4})}{\Gamma(-\frac{(\mu+\eta)^2}{2})} + \frac{(\mu+\eta)^2}{2} \frac{\psi(1 - \frac{(\mu+\eta)^2}{4}) - \psi(\frac{1}{2} - \frac{(\mu+\eta)^2}{4})}{\Gamma(1 - \frac{(\mu+\eta)^2}{2})} \right)$$

$$+ \frac{2^{\frac{(\mu-\eta)^2}{2}}\sqrt{\pi}}{4} \left(\frac{\psi(\frac{1}{2} - \frac{(\mu-\eta)^2}{4}) - \psi(-\frac{(\mu-\eta)^2}{4})}{\Gamma(-\frac{(\mu-\eta)^2}{2})} + \frac{(\mu-\eta)^2}{2} \frac{\psi(1 - \frac{(\mu-\eta)^2}{4}) - \psi(\frac{1}{2} - \frac{(\mu-\eta)^2}{4})}{\Gamma(1 - \frac{(\mu-\eta)^2}{2})} \right)$$

$$+ \frac{\left((\mu-\eta)^2 \Gamma^2(\frac{1}{2} - \frac{(\mu-\eta)^2}{4}) + 4\Gamma^2(1 - \frac{(\mu-\eta)^2}{4}) \right) \left(2\eta \Gamma(1 - \frac{(\mu+\eta)^2}{4}) + \Delta_0 \sqrt{1 - \frac{\eta^2}{\Delta_0^2}} (\eta + \mu) \Gamma(\frac{1}{2} - \frac{(\mu+\eta)^2}{4}) \right)^2}{4\Delta_0^3 \sqrt{1 - \frac{\eta^2}{\Delta_0^2}} (\mu-\eta)^2 \Gamma^2(\frac{1}{2} - \frac{(\mu-\eta)^2}{4}) \Gamma^2(1 - \frac{(\mu+\eta)^2}{4})}$$

$$g(\eta, \zeta) = \frac{\mu + \zeta}{\frac{(\mu+\eta)^2}{2} - \frac{(\mu+\zeta)^2}{2} + 1} \left(\frac{1}{\Gamma(\frac{1}{2} - \frac{(\mu+\eta)^2}{4}) \Gamma(\frac{1}{2} - \frac{(\mu+\zeta)^2}{4})} - \frac{1}{\Gamma(1 - \frac{(\mu+\zeta)^2}{4}) \Gamma(-\frac{(\mu+\eta)^2}{4})} \right)$$

$$G(\eta, \zeta) = \left(\frac{H_{\frac{(\mu+\eta)^2}{2}}(0) \frac{\eta}{\Delta_0} + (\mu + \eta) H_{\frac{(\mu+\eta)^2}{2}-1}(0) \sqrt{1 - \frac{\eta^2}{\Delta_0^2}}}{(\mu - \eta) H_{\frac{(\mu-\eta)^2}{2}-1}(0)} \right) \left(\frac{H_{\frac{(\mu+\zeta)^2}{2}}(0) \frac{\zeta}{\Delta_0} + (\mu + \zeta) H_{\frac{(\mu+\zeta)^2}{2}-1}(0) \sqrt{1 - \frac{\zeta^2}{\Delta_0^2}}}{(\mu - \zeta) H_{\frac{(\mu-\zeta)^2}{2}-1}(0)} \right),$$

where ψ and Γ denote the Digamma function and the Gamma function respectively [41].

straightforward Dirac notation, we have

Appendix E: Calculation of the envelope-function Hamiltonian using the Hellmann-Feynman theorem

The r.h.s of Eq. (6) in the main text lends itself to the application of the Hellman-Feynman theorem. Using a

$$\langle n''0 | \left[\frac{\partial \mathcal{H}(q)}{\partial q} \right]_{q=0} | n'0 \rangle = \langle n''0 | \left[\frac{\partial}{\partial q} \{ \mathcal{H}(q) | n'q \} - \mathcal{H}(q) \frac{\partial}{\partial q} | n'q \} \right]_{q=0}, \quad (\text{E1a})$$

$$= \langle n''0 | \left[\frac{\partial \varepsilon_{n'q}}{\partial q} \right]_{q=0} | n'0 \rangle + \langle n''0 | \{ \varepsilon_{n'0} - \mathcal{H}(0) \} \left[\frac{\partial}{\partial q} | n'q \rangle \right]_{q=0}, \quad (\text{E1b})$$

$$= \left[\frac{\partial \varepsilon_{n'q}}{\partial q} \right]_{q=0} \delta_{n''n'} + (\varepsilon_{n'0} - \varepsilon_{n''0}) \langle n''0 | \left[\frac{\partial}{\partial q} | n'q \rangle \right]_{q=0}. \quad (\text{E1c})$$

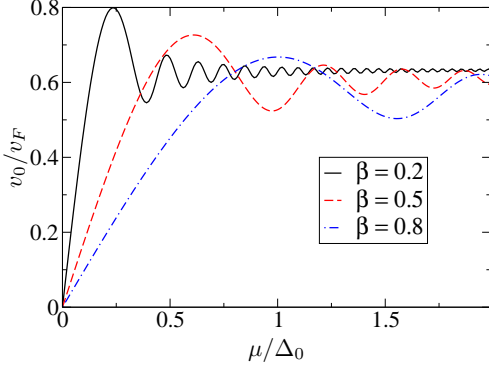


FIG. 5. Velocity of the Majorana mode along \hat{y} direction as a function μ/Δ_0 for different values of the magnetic field. $\beta \equiv \sqrt{\hbar|eB|}v_F/\Delta_0$ defines a dimensionless measure of the magnetic field. See the text for further details.

The expression given in Eq. (E1c) neatly separates the intra-band and inter-band matrix elements in the first and second terms, respectively. Inserting into Eq. (5) in the main text and using the definition Eq. (7) in the main text yields Eqs. (8) in the main text.

Naturally, the full matrix $H_{n''n'}(q)$ is not tractable. However, we are usually only interested in the bands in the vicinity of the chemical potential, as the relevant dynamics of the material will take place mostly in these. The coupling to more remote bands will affect the parameters in any reduced-band model (e.g., the effective mass in conventional semiconductor band models, or the velocity of the edge modes in our current system of interest). The systematic way to derive a reduced-band model is Löwdin partitioning (see, e.g., Appendix B in Ref. [42] for a pedagogical introduction).

Appendix F: Majorana mode coupled to nearest bands as an illustration of envelope-function theory

We will now consider the coupling of the Majorana mode ($n = 0$) to the nearest LLs (with $n = \pm 1$). The EF matrix Hamiltonian for this situation is given by (we use the notation $\bar{1} \equiv -1$)

$$\tilde{\mathcal{H}} = \begin{pmatrix} \hbar v_0 q & \varepsilon_1 A_{01} q & -\varepsilon_1 A_{0\bar{1}} q \\ -\varepsilon_1 A_{10} q & \varepsilon_1 + \hbar v_1 q & -2\varepsilon_1 A_{1\bar{1}} q \\ \varepsilon_1 A_{\bar{1}0} q & 2\varepsilon_1 A_{\bar{1}1} q & -\varepsilon_1 + \hbar v_{\bar{1}} q \end{pmatrix}, \quad (\text{F1})$$

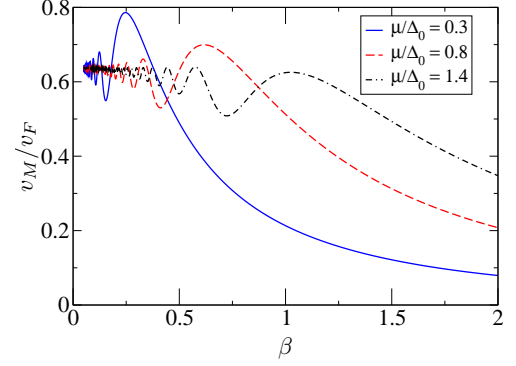


FIG. 6. Velocity of the Majorana mode along \hat{y} direction as a function of β for different values of μ/Δ_0 . See the text for further details.

where $\varepsilon_1 \equiv \varepsilon_{10} = -\varepsilon_{\bar{1}0}$. Straightforward diagonalization yields eigenvalues $\varepsilon_{\pm 1q} = \pm \varepsilon_1 + \hbar v_1 q + \mathcal{O}(q^2)$, $\varepsilon_{0q} = \hbar v_0 q + \mathcal{O}(q^2)$ and associated eigenstates $\chi_{nq} \equiv (a_{nq}^{(0)}, a_{nq}^{(1)}, a_{nq}^{(\bar{1})})^T$

$$\chi_{0q} = \begin{pmatrix} 1 \\ A_{10} q \\ A_{\bar{1}0} q \end{pmatrix}, \chi_{1q} = \begin{pmatrix} A_{01} q \\ 1 \\ A_{\bar{1}1} q \end{pmatrix}, \chi_{\bar{1}q} = \begin{pmatrix} A_{0\bar{1}} q \\ A_{1\bar{1}} q \\ 1 \end{pmatrix}, \quad (\text{F2})$$

also with accuracy of $\mathcal{O}(q^2)$. Thus, up to linear order in q , the inter-band coupling does not affect the linear dispersion of each mode, but an admixture between the different modes is present in the eigenstates.

We now consider the second-quantized representation of the Dirac-Andreev edge states. Based on the above discussion, we can write the annihilation operator for the state with wave number q in the $n = 0$ band as

$$\gamma_q = c_0 + q (A_{10} c_1 + A_{\bar{1}0} c_{\bar{1}}). \quad (\text{F3a})$$

Here c_n are the second-quantized operators associated with the $q = 0$ states in band n , i.e., our basis states. By the symmetry inherent to the Dirac-BdG equations, we have $c_0 = c_0^\dagger$ and $A_{\bar{1}0} c_{\bar{1}} \equiv -A_{10} c_1^\dagger$ and thus find

$$\gamma_q = c_0 + q A_{10} (c_1 - c_1^\dagger). \quad (\text{F3b})$$

Appendix G: Tuning the system properties via the external magnetic field

It should be noted that all the energy scales and momentum scales in Eq. (A3) are defined using the magnetic length thus removing any explicit dependence upon the external magnetic field. If we are interested in tuning the properties of our system by changing the external magnetic field, it is useful to define another set of dimensionless units where we can measure the strength of the magnetic field, this is achieved by measuring all the energies in units of the superconducting gap. We define $\tilde{\mu} \equiv \frac{\mu}{\Delta_0\beta}$, $\tilde{\varepsilon} \equiv \frac{\varepsilon}{\Delta_0\beta}$, $\tilde{q} \equiv \frac{\hbar v_F q}{\Delta_0\beta}$ where β is a dimensionless

measure of the magnetic field ($\beta \equiv \frac{\sqrt{\hbar|eB|}v_F}{\Delta_0}$). Using this Eq. (A3) can be rewritten as

$$f_{\tilde{\mu}+\tilde{\varepsilon}}(\tilde{q}) - f_{\tilde{\mu}-\tilde{\varepsilon}}(-\tilde{q}) = \frac{\beta\tilde{\varepsilon}(f_{\tilde{\mu}+\tilde{\varepsilon}}(\tilde{q})f_{\tilde{\mu}-\tilde{\varepsilon}}(-\tilde{q}) + 1)}{\sqrt{1 - \beta^2\tilde{\varepsilon}^2}}, \quad (\text{G1})$$

where the function $f_\alpha(q)$ is the same as defined earlier. Equation (G1) can be solved for $\tilde{\varepsilon}$. The numerical results for the velocity of the Majorana mode as a function of β and μ/Δ_0 is shown in Fig. 4 in the main text. In this supplemental material Fig. 5 shows v_0/v_F as a function of μ/Δ_0 for different values of β and similarly Fig. 6 shows v_0/v_F as a function of β for different values of μ/Δ_0 just to illustrate the oscillating behavior of v_0/v_F as seen in Fig. 4 in the main text.

-
- [1] F. Wilczek, *Nature Phys.* **5**, 614 (2009).
 - [2] J. Alicea, *Rep. Prog. Phys.* **75**, 076501 (2012).
 - [3] C. W. J. Beenakker, *Ann. Rev. Cond. Mat. Phys.* **4**, to appear (2013), preprint arXiv:1112.1950v2.
 - [4] M. Leijnse and K. Flensberg, preprint arXiv:1206.1736.
 - [5] E. Majorana, *Nuovo Cimento* **14**, 171 (1937).
 - [6] G. Moore and N. Read, *Nucl. Phys. B* **360**, 362 (1991).
 - [7] A. Stern, *Nature* **464**, 187 (2010).
 - [8] D. A. Ivanov, *Phys. Rev. Lett.* **86**, 268 (2001).
 - [9] A. P. Mackenzie and Y. Maeno, *Rev. Mod. Phys.* **75**, 657 (2003).
 - [10] J. D. Sau, R. M. Lutchyn, S. Tewari, and S. Das Sarma, *Phys. Rev. Lett.* **104**, 040502 (2010).
 - [11] J. D. Sau, S. Tewari, R. M. Lutchyn, T. D. Stanescu, and S. Das Sarma, *Phys. Rev. B* **82**, 214509 (2010).
 - [12] J. Alicea, *Phys. Rev. B* **81**, 125318 (2010).
 - [13] M. Z. Hasan and C. L. Kane, *Rev. Mod. Phys.* **82**, 3045 (2010).
 - [14] X.-L. Qi and S.-C. Zhang, *Rev. Mod. Phys.* **83**, 1057 (2011).
 - [15] K. Sengupta, I. Žutić, H.-J. Kwon, V. M. Yakovenko, and S. Das Sarma, *Phys. Rev. B* **63**, 144531 (2001).
 - [16] C. J. Bolech and E. Demler, *Phys. Rev. Lett.* **98**, 237002 (2007).
 - [17] K. T. Law, P. A. Lee, and T. K. Ng, *Phys. Rev. Lett.* **103**, 237001 (2009).
 - [18] K. Flensberg, *Phys. Rev. B* **82**, 180516 (2010).
 - [19] V. Mourik, K. Zuo, S. M. Frolov, S. R. Plissard, E. P. A. M. Bakkers, and L. P. Kouwenhoven, *Science* **336**, 1003 (2012).
 - [20] A. Das, Y. Ronen, Y. Most, Y. Oreg, M. Heiblum, and H. Strikman, preprint arXiv:1205.7073.
 - [21] L. Fu and C. L. Kane, *Phys. Rev. Lett.* **100**, 096407 (2008).
 - [22] L. Fu and C. L. Kane, *Phys. Rev. Lett.* **102**, 216403 (2009).
 - [23] A more detailed theoretical treatment of these effects can be developed along the lines of previous studies [37, 38].
 - [24] A. R. Akhmerov and C. W. J. Beenakker, *Phys. Rev. Lett.* **98**, 157003 (2007).
 - [25] See Supplemental Material at <http://link.aps.org/supplemental/XXX>.
 - [26] H. Hoppe, U. Zülicke, and G. Schön, *Phys. Rev. Lett.* **84**, 1804 (2000).
 - [27] P. G. de Gennes, *Superconductivity of Metals and Alloys* (Addison-Wesley, Reading, MA, 1989).
 - [28] The operator $\Xi = \sigma_y \otimes \tau_y \mathcal{K}$ represents particle-hole conjugation in Nambu space [21]. τ_y is a Pauli matrix acting in Nambu space and \mathcal{K} symbolizes complex conjugation.
 - [29] See, e.g., Sec. 5.6 in U. Rössler, *Solid State Theory: An Introduction*, 2nd ed. (Springer, Berlin, 2009).
 - [30] More information on the Hellmann-Feynman theorem can be found in quantum-physics textbooks, e.g., Complement G_{XI} 5.b of Ref. 39.
 - [31] The introduction of a cut-off scale $\Lambda \sim l_B^{-1}$ and normalization factor \mathcal{N}_Λ is necessitated by the limited range in q over which the $n = 0$ -mode dispersion is linear.
 - [32] S. A. Kivelson and D. S. Rokhsar, *Phys. Rev. B* **41**, 11693 (1990).
 - [33] C. Nayak, K. Shtengel, D. Orgad, M. P. A. Fisher, and S. M. Girvin, *Phys. Rev. B* **64**, 235113 (2001).
 - [34] K. Fujita, I. Grigorenko, J. Lee, W. Wang, J. X. Zhu, J. C. Davis, H. Eisaki, S. Uchida, and A. V. Balatsky, *Phys. Rev. B* **78**, 054510 (2008).
 - [35] S. A. Parameswaran, S. A. Kivelson, R. Shankar, S. L. Sondhi, and B. Z. Spivak, preprint arXiv:1202.3444.
 - [36] I. Petkovic, F. I. B. Williams, K. Bennaceur, F. Portier, P. Roche, and D. C. Glatthil, *ArXiv e-prints* (2012), arXiv:1206.2940.
 - [37] U. Zülicke, H. Hoppe, and G. Schön, *Physica B* **298**, 453 (2001).
 - [38] F. Giazotto, M. Governale, U. Zülicke, and F. Beltram, *Phys. Rev. B* **72**, 054518 (2005).
 - [39] C. Cohen-Tannoudji, B. Diu, and F. Lalöë, *Quantum Mechanics*, Vol. II (Wiley, New York, 1977).
 - [40] C. W. J. Beenakker, *Phys. Rev. Lett.* **97**, 067007 (2006).
 - [41] I. S. Gradshteyn and I. M. Ryzhik, *Table of Integrals, Series, and Products* (Academic Press, San Diego, 1994), 5th ed.
 - [42] R. Winkler, *Spin-Orbit Coupling Effects in Two-Dimensional Electron and Hole Systems* (Springer, Berlin, 2003).